Sensors & Transducers, Vol. 173, Issue 6, June 2014, pp. 215-223

Sensors & Transducers

http://www.sensorsportal.com

Inorganic and Organic Screen-printed Cantilever-based Gas Sensors

[1] Hélène DEBEDA, [1] Riadh LAKHMI, [1, 2] Pierrick CLEMENT, [2] Eduard LLOBET, [3] Carlos Ruiz ZAMARRENO, [3] Francisco Javier ARREGUI and [1] Claude LUCAT

[1] Université Bordeaux, IMS Laboratory, 351 Cours de la Libération Talence, 33405, France
[2] Universitat Roviri I Virgili, Emas Research Center, Avenido Paisos Catalan, 43007 Tarragona, Spain
[3] Universitat Publica Navarra, Campus Arrosadia, 31006 Pamplona, Spain
Tel.: +33 540 00 83 36, fax: +33 556 37 15 45
[1] E-mail: helene.debeda@ims-bordeaux.fr

Received: 1 June 2014 /Accepted: 27 June 2014 /Published: 30 June 2014

Abstract: Researches on microcantilever MEMS are numerous in different areas, physical or chemical sensing, actuation or energy harvesting. Because of their high sensitivity at room temperature, they have been shown to be interesting for gas detection. Though silicon technology allows the processing of such cantilevers, alternative technologies are also attractive and have been developed for a few years. Potential achievement of organic and inorganic thick-film cantilevers is studied, through the association of the sacrificial layer process to the well-known screen-printing technology used for the fabrication of low cost components and microsystems. Epoxy-type, gold and resonant piezoelectric Au/PZT/Au cantilevers with or without coating have been successfully tested under humidity, toluene and benzene. The potentiality of the screen-printing technology for the development of cantilever-based gas sensors is demonstrated. *Copyright © 2014 IFSA Publishing, S. L.*

Keywords: Cantilevers, Humidity and VOC detection, Sacrificial layer, Screen-printing.

1. Introduction

The microsystems, generally designated by MEMS (Micro-Electro-Mechanical Systems), have been used for some years in the fields of micro-electronics, microrobotics, microfluidics, etc. For their processing, silicon-based materials are the mainly used ones. Related manufacturing approaches are derivated from microfabrication processes developed for integrated circuits. Nowadays, development of new polymer based-MEMS is attractive considering their low cost, good processability and bio-compatibility [1]. Other alternative technologies such as LTCC [2, 3] or direct prototyping processes (inkjet, micropen, microstereolithography, etc.) can also be used because of the microstructuration potentiality of different materials (polymers, composites, metals, ceramics) on different substrates. Moreover, association of these technologies with micromachined silicon is likely to be more and more considered for MEMS fabrication in the future [4]. The low cost screen-printing processing is also considered for the fabrication of hybrid MEMS. This technology, mainly used in microelectronics for interconnections and packaging purposes [5], has been extended to development of passive components such as sensors [6] and more recently to inorganic material-based MEMS or polymer-based microfluidic or micromechanical devices by using a sacrificial layer [7-9]. The choice of such technology for MEMS fabrication is justified because of the large choice of substrates, starting materials, layers geometries, multi-layers deposition and the control of the layer's porosity. Its simplicity, reliability, collective fabrication at low cost and the possibility of hybrid MEMS integration or coupling with others technologies (LTCC, ink jet, …), are also attractive.

Among MEMS, microcantilevers are common structures, highly sensitive, employed for different applications such as mechanical and gas sensors, AFM, etc. Silicon cantilever based sensors are particularly attractive for gas sensing because of their high sensitivity at room temperature [10-13]. To perform detection of chemical species, in gas or liquid media, the microcantilever is usually coated with a chemically sensitive layer that aims to selectively sorb the target analyte. The sorbed species modify the mechanical properties of the sensitive coating, inducing a change in the mass, the rigidity and the surface stress of the cantilever. The sorbed species can consequently be detected by measuring either the microcantilever's resonant frequency shift in the dynamic mode or its quasi-static deflection in the static mode [14].

In this work, screen-printing technology associated to a sacrificial layer is proposed for the fabrication of organic or inorganic based cantilevers on an alumina substrate, used for gas detection in static or dynamic mode. Because of its low Young's modulus, the organic cantilever will be preferred for cantilever-based sensors used in the static mode. The inorganic layers, especially those having an integrated piezoelectric actuation, are dedicated to the dynamic mode. Metallic, piezoelectric and epoxy based-cantilevers are achieved using the original processes developed at IMS laboratory for the fabrication of free-standing components and microsystems. The influence of the thermal treatment on the mechanical and electrical properties of the cantilevers is studied. In order to demonstrate screen-printing process potentialities for gas sensor applications, humidity, toluene and benzene detection are performed on uncoated and coated cantilevers.

2. Cantilever-based Sensors Fabrication

2.1. Screen-printing Associated to Sacrificial Layer Process

The screen-printing process described in Fig. 1 requires specific inks made of powder and organic binder mixed together. These inks are transferred onto the substrate with a squeegee, through open meshes areas of the patterned screen. Then, the deposited film is dried and cured at low temperatures (<250 °C) if it is a polymer paste or fired at high temperature (400 to 1100 °C) in the case of mineral paste for sintering and adherence of the thick film on the substrate. The curing of polymer-based pastes allows solvent evaporation and chains cross linking of the thermosetting resin giving the polymer its mechanical properties. The firing of mineral-based inks performed at temperatures between 400 °C and 1100 °C favors the sintering of the mineral powder.

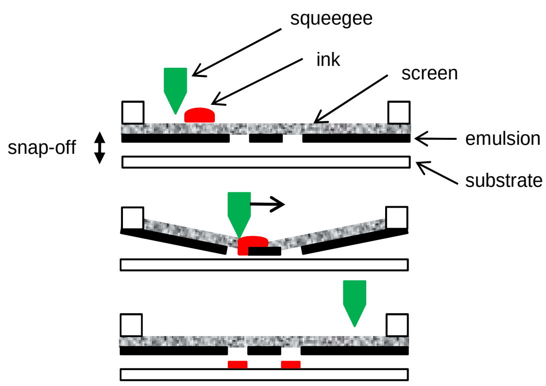

Fig. 1. Screen-printing process.

To generate movable microstructures in an integrated process, it is necessary to use a substrate with a pre-patterned sacrificial layer. The main sacrificial layer requirements are hardness and chemical compatibility for easy removal without substrate or other layers damage. The sacrificial layer technique has already been successfully used in silicon micromachining but also in alternative technologies such as LIGA, ink-jet and polymer MEMS processing [15, 16], with the adapted deposition techniques (evaporation, sputtering, spin-coating, electroplating, printing). For screen-printed polymer structures, interesting results have been obtained with ethylcellulose and silicon resins for channels and cantilevers fabrication where the sacrificial layer sublimates at 150 °C without any degradation of the structural layer [8]. Concerning mineral screen-printed movable structures, carbon, metal or glass based sacrificial layers are used but are not always satisfactory [17-19]. These authors underline that glass, metal or carbon based sacrificial layers give rise to thick-film deformations. In order to overcome this problem, specific screen-printed sacrificial layer as well as the optimized thermal treatment is selected for our organic and inorganic processes.

2.2. Inorganic Cantilevers Processing

2.2.1. Gold Cantilevers

The sacrificial layer is made of epoxy resin blended with strontium carbonate $SrCO_3$ powder. Indeed, among numerous potential materials for sacrificial layer, $SrCO_3$ appears to be a good compromise with regard to thermal stability, melting point, solubility in weak acidic solutions, toxicity, etc.., to be used as basic material of the sacrificial layer in the fabrication process of screen-printed MEMS [7]. The epoxy matrix gives the hardness of the sacrificial deposition for further structural layer depositions. The first free-standing thick-films are achieved with gold cantilevers on an alumina substrate (Fig. 2).

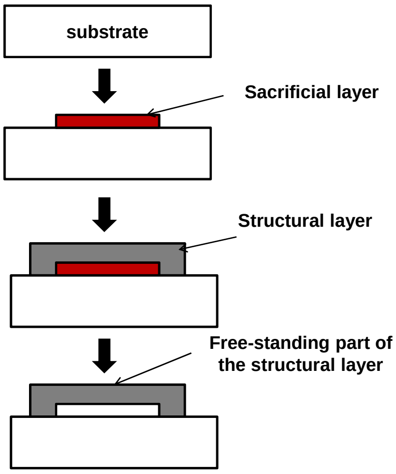

(a)

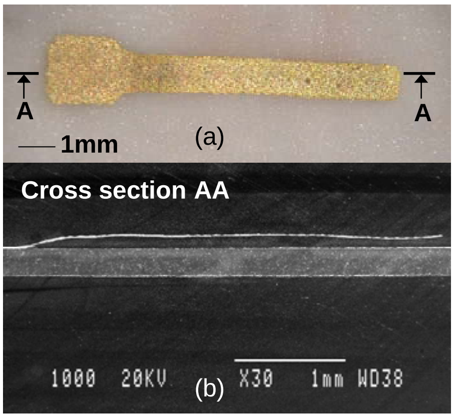

(b)

Fig. 2. Sacrificial layer based screen-printing process for free-standing layer fabrication (a) and photograph of gold cantilever (b).

The sacrificial layer (epoxy $+SrCO_3$) is printed and polymerized 20 min at 120 °C prior to depositions of a gold pad and a gold cantilever, regarding a curing step of 25 min at 120 °C between each layer deposition. The $SrCO_3$ paste is made at the laboratory whereas the gold paste (ESL8836) is commercialized by ESL (ElectroScience Laboratories). After printing, the sample is fired under air atmosphere according to the temperature profile of Fig. 3. The onset temperatures of epoxy pyrolysis and of $SrCO_3$ decomposition are around 300-450 °C and 850 °C respectively. During the firing process, the first plateau (8 min at 450 °C) allowing the whole epoxy degradation is followed by the gold sintering taking place with the second plateau (15 min at 850 °C). After the thermal treatment, the sample is finally immersed in a 0.9 mol.l-1 H_3PO_4 aqueous solution to dissolve the remaining $SrCO_3$ sacrificial layer. Energy-dispersive X-ray analyses demonstrate the harmlessness and the efficiency of the process for the fabrication of a cantilever-type structure. Indeed, no diffusion of any chemical element from the sacrificial layer towards the Au structural layer is detected. The process has also been applied to the fabrication of microsystems such as force or catalytic gas sensors, thermal actuators or free-standing resonators based on screen-printed piezoelectric layers. Copper and silver as well as vitroceramic free-standing cantilevers have been for example successfully processed for thermal actuators [20] and force sensors [21] respectively, without bending. Hence, the compatibility between the $SrCO_3$ sacrificial layer and different structural layers has been demonstrated.

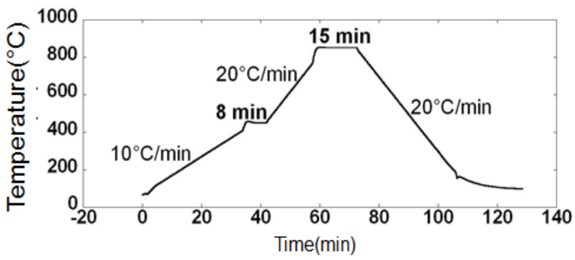

Fig. 3. Temperature profile optimized for gold cantilevers sintering.

2.2.2. Piezoelectric PZT Cantilevers

The piezoelectric cantilevers based on $PbZr_{0.52}Ti_{0.48}O_3$ (PZT) material from Ferroperm is a multilayer structure composed of the PZT sandwiched between two gold electrodes (Au/PZT/Au) (Fig. 4(a)). For such multilayer cantilever structures, important deformations of the cantilevers or electrodes delaminations may appear at the end of the process mainly if the thermal expansion coefficients do not match well [9]. In our case, cantilever's deformations observed in some samples does not come from thermal expansion mismatch but essentially from sacrificial layer swelling when the sample is dipped into the acidic solution. Gold (ESL8836) based electrode is selected because of its compatibility with the $SrCO_3$ sacrificial layer and its good adhesion and minor diffusion inside the PZT layer, as demonstrated with a Au/PZT/Au bridge structure [22]. Concerning the piezoelectric paste, 3 %wt of the eutectic phase $Li_2CO_3/Bi_2O_3/CuCO_3$ is added to decrease their sintering temperature [23]. The multilayer structure of the cantilevers implies a co-firing only at the end of the deposition of the different structural layers, due to the sacrificial layer's brittleness after firing.

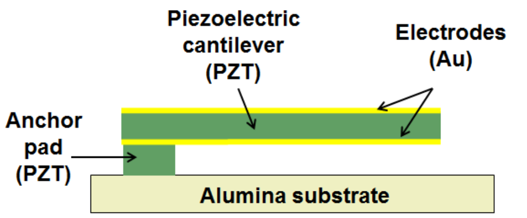

(a)

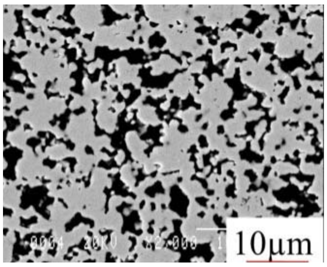

(b)

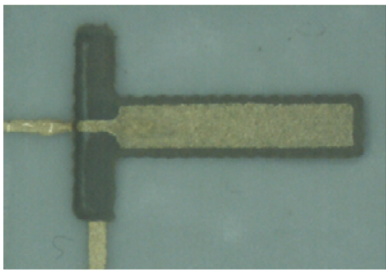

(c)

Fig. 4. Cantilever structure (a), SEM photograph of the PZT layer (b) and cantilever photograph (c).

The anchor pad made of PZT is first screen-printed on the alumina substrate and dried 20 min at 120 °C. Then, the sacrificial layer is deposited on the alumina substrate and polymerized 20 min at 120 °C. Finally, bottom gold electrode, PZT layer and top gold electrode are printed successively, with a drying step at 120 °C during 20 min between each deposition. To improve the densification and thus electrothermal properties [23], the samples are isostatically pressed 1 min at 1 kbar before firing. Afterwards, the samples are co-fired 2 hours in air atmosphere with a similar profile as for gold cantilevers except the sintering plateau, lasting 2 hours at 900 °C to reduce the layer porosity (Fig. 4(b)). At the end, the removal of the sacrificial layer is performed in the phosphoric acid aqueous solution (Fig. 4(c)). Finally, the Au/PZT/Au cantilevers are poled under 50 kV/cm at 280 °C, just below the PZT's Curie temperature. After poling, piezoelectric properties are extracted from impedance and capacitance measurements using an HP 4194A impedance analyzer. Three resonance peaks shown on Fig. 5 are related to the three first in-plane 31-longitudinal vibration modes (31 refers to the piezoelectric effect: the electrical polarization is perpendicular to the mechanical displacement).

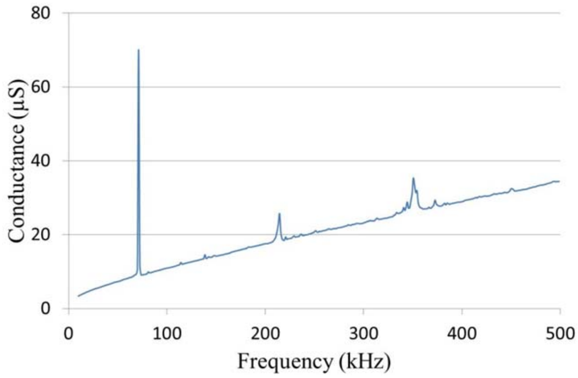

Fig. 5. Conductance measurements for the 2×8×0.1 mm^3 PZT cantilever.

2.3. Organic Cantilevers Processing

Based on the inorganic process allowing the fabrication of Au or Au/PZT/Au cantilevers, epoxy based cantilevers are structured but in this case using a whole polymer sacrificial layer. Polyester material is selected as a sacrificial layer because it can be dissolved in acetone solution at room temperature without affecting the epoxy structural layer. The different fabrication steps of the initial screen-printing fabrication process of epoxy-based cantilevers are summarized in Fig. 6. Note that a commercial composite ink from ESL (RS12113) made of epoxy resin and carbon powder is chosen for the structural layer. This resistive composition can be later used for strain gauges fabrication in a bilayer sensor working as static cantilever.

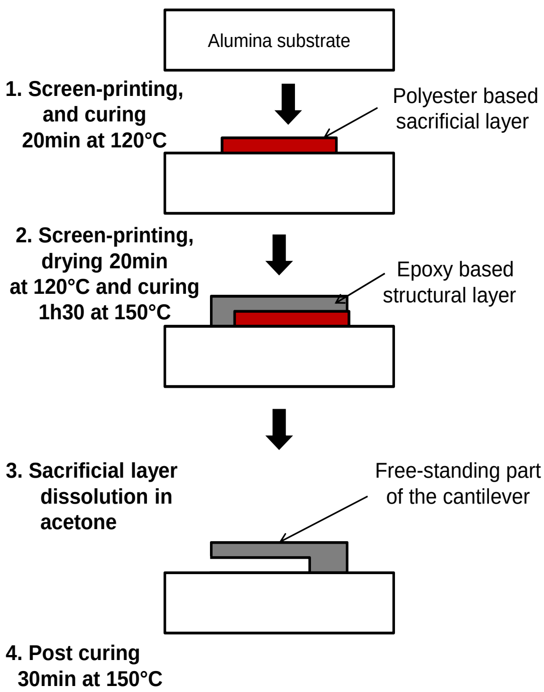

Fig. 6. Initial processing of the screen-printed epoxy cantilever.

Because most of the first epoxy cantilevers exhibit up-curvature when cured in the oven at 150 °C, improvement of the organic cantilevers' curing process is undertaken in order to obtain flat cantilevers parallel to the substrate. For this purpose, a vapor-phase equipment dedicated to solder paste reflow at 230 °C is used. Compare to the oven process, the thermal exchanges between the cantilever and the vapor phase are more efficient leading to a more homogeneous temperature. The influence of the curing process on the final shape of the organic cantilever is reported in the Table 1. A possible source of the deformation observed for the samples directly introduced in the oven at 150 °C is the rapid elimination of the solvent contained in the epoxy-based ink. In the same way, curing in an oven from room temperature to 150 °C with a heating rate of 1.5 °C, min-1 do not lead to satisfactory results. In this case, the sacrificial layer removal is difficult because of possible chemical reaction between the polyester sacrificial layer and the epoxy layer. In the case of the vapor-phase process, it is shown that a curing ramp of 0.8 $°C.s^{-1}$, followed by the sacrificial layer dissolution and post-curing of 30 min at 150 °C, allows a better control of the cantilevers' shape whatever their thickness (20 to 80 μm). On Fig. 7 are shown the different sizes of non deformed cantilevers. (Fig. 7(b)) shows the effect of air stream on one of the vapor-phase cured cantilevers, recovering its initial position when air stream is turned off. This vapor phase curing gives satisfactory results in terms of cantilever geometry. Mechanical and electrical characterizations reveal that the polymerization process is completed. For this purpose, the resistance of epoxy layers directly printed on the alumina substrate is measured all along the curing phase. In the case of samples cured in the oven, resistance drifts are still observed at the end of the process whereas the resistance is stable for vapor phase curing. Concerning the mechanical properties, Dynamic Mechanical Analysis (DMA) is performed with a rheometer system analyzer (RSA3) which permits evaluation of the Young's Modulus E ~1.9GPa and of the glass transition temperature T_g ~174°C corresponding to the dielectric losses' peak. This later has been chosen as a criteria to determine the degree of polymerization. It is shown that the oven cured samples are not completely polymerized. Indeed, for 3 consecutive DMA tests performed, an evolution of the dielectric losses' peak is observed conversely to the samples cured in vapor-phase where no shift appears.

3. Gas Detection with Uncoated Cantilevers

In order to prevent from ageing phenomena linked to the sensitive layer, cantilevers operating in dynamic mode can be used without any coating. In this case, resonant frequency shifts Δf_r can be justified by viscosity and density effects of the gas surrounding the resonant cantilevers [24], but also by sorption effect in the screen-printed layers modifying both the cantilever's mass and the stiffness according to the relation:

$$\Delta f_r = \frac{f_r}{2}\left(\frac{\Delta k}{k} - \frac{\Delta m}{m}\right), \tag{1}$$

where f_r is the resonant frequency, m is the cantilever's mass and k is the cantilever's stiffness.

Uncoated gold cantilevers and Au/PZT/Au cantilevers have been tested under gas. For gold cantilevers, a piezoelectric ceramic placed under the cantilevers allows an external actuation of the cantilever vibrating out of plane with the bending mode (Fig. 8(a)). The resonance frequency is measured optically using a laser vibrometer (Polytec MSA 500). For piezoelectric cantilevers, the structure is self-actuated thanks to the simple Au/PZT/Au structure also used at the same time to perform the mechanical signal transduction. Because of their symmetric structure, the PZT-based cantilevers are vibrating in the plane (Fig. 8(b)) contrarily to gold cantilevers.

Both cantilevers have been tested under humidity produced by a vapor generator cell (VGI MEMS from Surface Measurement Systems) operating with a nitrogen gas flow. Results show a good reversibility of the sorption without any resonant frequency drifts (Fig. 9).

Table 1. Influence of the curing profile on the epoxy cantilever deformation

Equipment	**Temperature ramp**	**Peak temperature**	**Plateau duration**	**Cantilevers' photographs ($2\times8\times 0.08\ mm^3$)**
Oven	Direct introduction at 150 °C	150 °C	2 h	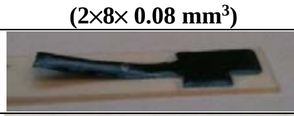
	$1.5\ °C.min^{-1}$	150 °C	30min	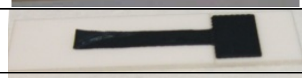
Vapor phase	$0.6\ °C.s^{-1}$	230 °C	1 min	
	$0.8\ °C.\ s^{-1}$	230 °C	4 min	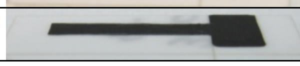

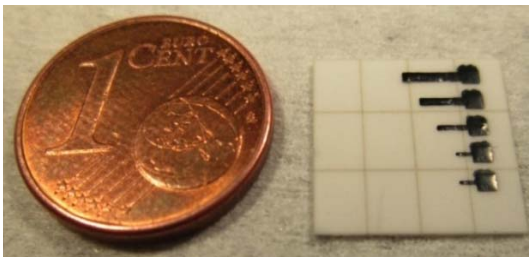

(a) 1 mm×220 µm, 2 mm×400 µm, 3 mm×600 µm, 4 mm×800 µm cantilevers

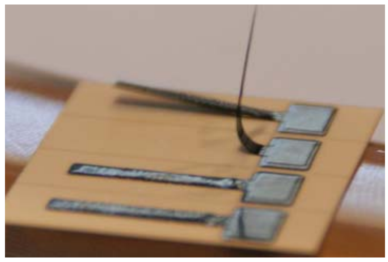

(b) 8×2 mm² cantilever under air stream

Fig. 7. Photograph of 20 µm thick epoxy cantilevers of different sizes.

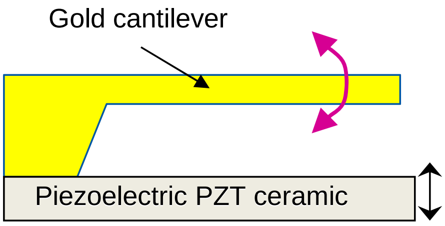

(a)

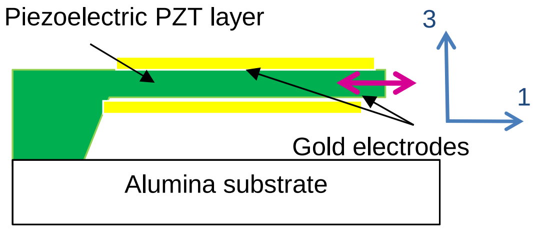

(b)

Fig. 8. Actuation of the gold and Au/PZT/Au cantilevers.

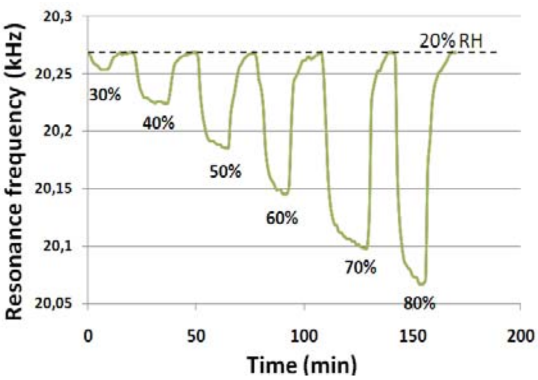

(a) Gold cantilever 2×8×0.05 mm^3 in the out-of-plane bending mode.

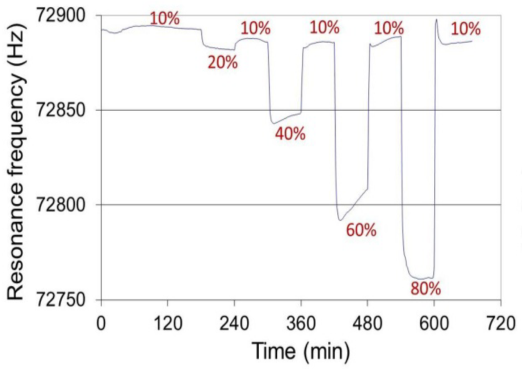

(b) Au/PZT/Au cantilever 2×8×0.1 mm^3 in the in-plane 31-longitudinal mode.

Fig. 9. Resonance frequency shifts under humidity for uncoated Au cantilevers (a) and PZT cantilevers.

Sensitivity of 1.7 Hz/%RH is calculated for the 8×2×0.05 mm^3 Au cantilever in bending mode. In the case of 8×2×0.08 mm^3 Au/PZT/Au cantilevers, values of 1.9 Hz/%RH are observed. For 80 % RH, resonance frequency shifts of more than 100 Hz are obtained for Au and Au/PZT/Au cantilevers whereas inertial and viscous effect of humidity would theoretically induce frequency variations lower than 0.1 Hz [25].

Conversely to uncoated silicon-cantilevers where gas inertial and viscous effects are sufficient to explain the amplitude and sign of the frequency shifts, those effects do not explain the resonance frequency shifts observed in our case. The negative shifts obtained can be explained by a predominance of mass effect, attributed to the porosity of the screen-printed layers.

4. Gas Detection with Coated Cantilevers

4.1. PZT Cantilevers Coated with PEUT

The Au/PZT/Au cantilevers are tested under toluene. For this purpose, the polymer PEUT PolyEtherUreThane is chosen because of its good partition coefficient to toluene (K=1610). It is deposited with a dispenser on the surface of the cantilevers (thickness~30 µm) for toluene detection. Then, the PEUT-functionalized cantilevers are placed under a controlled nitrogen flow (100 mL/min) and tested under different toluene concentrations (Fig. 10). Good reproducibility and linearity of the response is observed. Table 2 summarizes the sensors' performance towards toluene of screen-printed Au/PZT/Au cantilevers and those of standard Si cantilevers having also millimeter sizes. Toluene detection performances are similar for both types of cantilevers. Our self-excited and integrated read-out PZT cantilevers coated with a 30 µm PEUT sensitive layer are very sensitive to toluene (48 mHz/ppmV). Compared to Si cantilevers coated with PEUT, the PZT-based cantilevers present higher sensitivities but the Limit Of Detection (LOD) is limited by the lower quality factor, inducing higher signal noise.

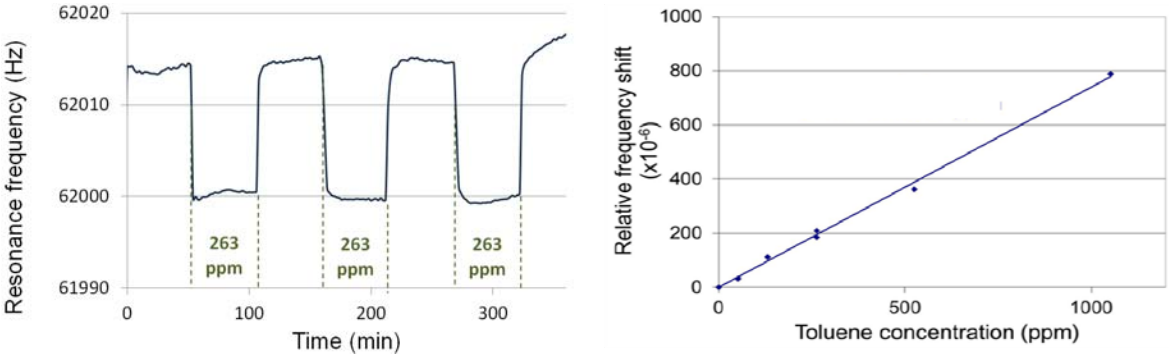

(a) (b)

Fig. 10. Tests under toluene with a 30µm PEUT-coated PZT cantilever (8×2×0.1 mm^3), a) resonant frequency shift of the 1st 31-longitudinal mode under different concentrations, and b) repeatability to 263 ppm.

Table 2. Toluene detection with Si and PZT cantilevers functionalized with PEUT

Cantilever type	Resonant frequency f_r/mode	Quality factor Q	Sensitivity $S_{CA} = \left\lvert \frac{df_r}{dC_A} \right\rvert$ (10^{-4}Hz.ppmV^{-1})	Normalized sensitivity $S_{CA}/f_r/h_{PEUT}$ (10^{-6}ppm.V^{-1}. mm^{-1})	Noise (mHz)	Limit Of Detection LOD = $3\Delta f_{noise}/S_{CA}$ (ppmV)
Si (5×0.4×0.06 mm^3) h_{PEUT}= 18 µm	3 kHz /out-of-plane flexural	940	9	16	14	16
PZT (8×2×0.10 mm^3) h_{PEUT}= 30 µm	62 kHz/in-plane longitudinal	150	478	25.7	400	25

4.2. PZT Cantilevers Coated with Active Carbon

To increase the sensitivity to Volatile Organic Compounds (VOC's), polymer sensitive coating can be replaced by inorganic nanoporous coatings like zeolite exhibiting higher sensitivity [26] or active carbon.

Active carbon with high surface area (1779 m^2 g^{-1}) and small pore width (1 nm for a particle size of 5 µm) is selected for its high adsorption capacity of VOC's. Active carbon coating process consists of drop coating with a micro-dispenser of the active porous carbon suspension, followed by solvent evaporation at 125 °C and a thermal annealing at 250 °C (Fig. 11(a). A sensitivity of 13 Hz/ppmV under benzene is measured, for a ~20 µm coating (Fig. 11(b)).

4.3. Epoxy Cantilevers Coated with Agarose

Detection of humidity with epoxy cantilevers is performed. For this purpose, the agarose hydrogel, already used for humidity detection with optical fibers sensors, is selected [27]. It is deposited on the top cantilever with a syringe, prior to a plasma pre-treatment of the epoxy in order to obtain a hydrophilic surface. The functionalized cantilevers are finally tested under humidity. During this stage, the swelling of agarose under humidity leads to a bending of the bilayer cantilever. Hence, the deflection of the cantilever's tip is measured with an optical profilometer (Altisurf 500) at room temperature for different humidity rates. The deflection measurements show a good reproducibility and reversibility of the sensor response with sensitivity of 4.6 µm/%RH (Fig. 12).

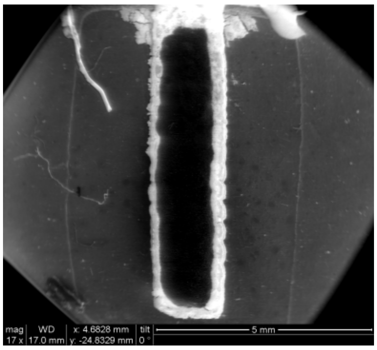

(a)

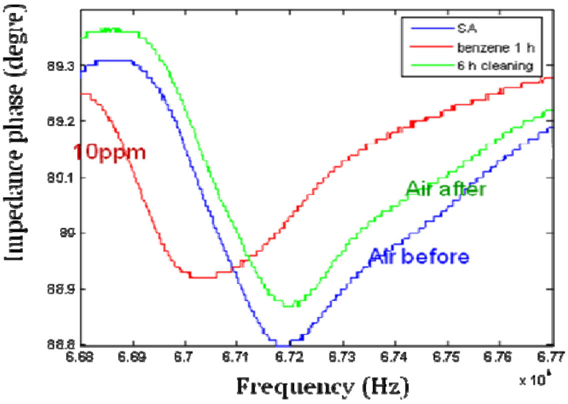

(b)

Fig. 11. Tests Photograph of the screen-printed PZT cantilever coated with active carbon (a) and impedance measurements under air and 10 ppm benzene (b).

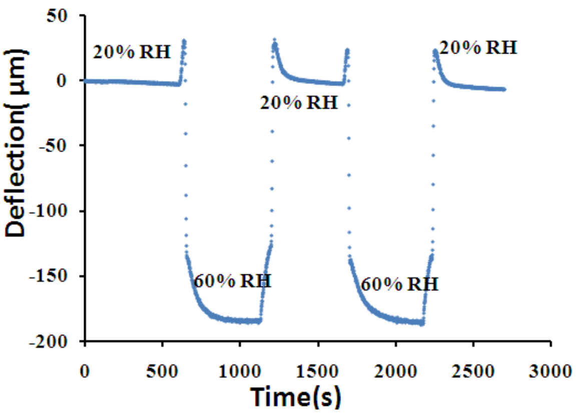

Fig. 12. Deflection of the tip's cantilever ($2.5\times10\times0.08$ mm^3) measured under humidity.

5. Conclusions

The thick-film sacrificial layer process described in this paper may well open new routes of investigation for MEMS microfabrication, complementary to silicon, LTCC or PCB ones. The efficiency of this simple and low cost process is demonstrated through the fabrication of organic and inorganic-based cantilevers for gas sensors applications. Au/PZT/Au and gold cantilevers are sensitive to humidity. Concerning PEUT and active carbon coated piezoelectric cantilevers, a good sensitivity is measured at low concentrations of toluene and benzene respectively. Likewise, preliminary experiments with epoxy-based sensors coated with agarose show the capability of organic screen-printed cantilevers for humidity detection.

Moreover, the self-actuated Au/PZT/Au cantilevers can also be promising for species detection in liquid media, even if the quality factor in air is smaller than those of the transverse bending mode of silicon-based microcantilevers. Indeed, when immersed in viscous fluids, the decrease of the quality factor is very low (from 400 to 20 from air to fluid of viscosity 500 cP) for these self-actuated piezoelectric cantilevers vibrating with the in-plane 31-longitudinal mode compared to silicon cantilevers [28].

Acknowledgements

The authors would like to thank Région Aquitaine, Generalitat de Catalunya, and Gobierno de Navarra for having supported these researches through the CTP Project entitled "Piezoelectric microsystem functionalized with nano powders for the selective detection of Volatil Organic Compounds". They wish also to thank the engineer E. Ibarboure from the LCPO Laboratory, Université Bordeaux, Talence, France for DMA measurements.

References

[1]. C. Liu, Foundations of MEMS, Illinois ECE Series, *Pearson Prentice Hall*, 2006.

[2]. J. J. Santiago-Avilés, M. R. Gongora-Rubio, P. Espinoza-Vallejos and L. Sola-Laguna, Sensors, actuators and other non-packaging applications of LTCC tapes, in *Proceedings of the IMAPS Conference on Ceramic Interconnect Technology (IMAPS-CICMT'04)*, Denver, 2004, pp. 7-12.

[3]. H. Birol, T. Maeder and P. Ryser, Processing of graphite-based sacrificial layer for microfabrication of low temperature co-fired ceramics (LTCC), *Sensors and Actuators A,* Vol. 130–131, 2006, pp. 560–567.

[4]. H. Zhu, J. Miao, Z. Wang, C. Zhao and W. Zhu, Fabrication of ultrasonic arrays with 7 µm thick films as ultrasonic emitter for object detection in air, *Sensors and Actuators A*, Vol. 123-124, 2005, pp. 614-619.

[5]. M. Haskard and K. Pitt, Thick film technology and applications, *Electrochemical Publications*, 1997.

[6]. F. Ménil, H. Debéda, C. Lucat, Screen-printed thick-films: from materials to functionnal devices, *Journal of European Ceramic Society*, Vol. 25, Issue 12, 2005, pp. 2105-2113.

[7]. C. Lucat, P. Ginet, C. Castille, H. Debéda and F. Ménil, Microsystems elements based on free-standing thick-films made with a new sacrificial layer

process, *Microelectronics Reliability*, Vol. 48, Issue 6, 2008, pp. 872-875.

[8]. N. Serra, T. Maeder, O. Gentsch and P. Ryser, Fabrication of polymer-based micro devices: formulation and study of the paste, *Sensors and Actuators A*, Vol. 172, 2011, pp. 336-340.

[9]. S. Kok, N. M. White and N. R. Harris, Fabrication and characterization of free-standing thick film piezoelectric cantilevers for energy harvesting, *Measurement Science and Technology*, Vol. 20, No. 12, 2009, Article ID 124010.

[10]. K. M. Goeders, J. S. Colton and L. A. Bottomley, Microcantilevers: sensing chemical interactions via mechanical motion, *Chemical Reviews*, Vol. 108, Issue 2, 2008, pp. 522-542.

[11]. A. Boisen, S. Dohn, S. S. Keller, S. Schmid and M. Tenje, Cantilever-like micromechanical sensors, *Reports on Progress in Physics*, Vol. 74, 2011, pp. 1-31.

[12]. X. Li and D. W. Lee, Integrated microcantilevers for high-resolution sensing and probing, *Measurement Science and Technology*, Vol. 23, Issue 2, 2012, Article ID 022001, 40 pages.

[13]. M. Sepaniak, P. Datskos, N. Lavrik and C. Tipple, Microcantilever transducers: A new approach in sensor technology, *Analytical Chemistry*, 74, 2002, pp. 568-575.

[14]. S. Srikanth Singamaneni, M. C. Lemieux, H. P. Lang, C. Gerber, Y. Lan, S. Zauscher, P. G. Datkos, N. V. Lavrik, H. Hiang, R. R. Naik, T. J. Bunning and V. V. Tsukruk, Bimaterial microcantilevers as a hybrid sensing platform, *Advanced Materials*, Vol. 20, Issue 4, 2008, pp. 653-680.

[15]. F. Yi, E. Tang, J. Zhang and D. Xian, A new sacrificial layer method of LIGA technology to fabricate movable part of a gripper, *Microsystems Technologies*, Vol. 6, Issue 4, 2000, pp. 154-156.

[16]. P. Abgrall, V. Conedera, H. Camon, A.-M. Gué and N.-T. Nguyen, SU-8 as a structural material for labs-on-chips and micromechenical systems, *Electrophoresis*, Vol. 28, 2007, pp. 4539-4551.

[17]. G. Stecher, Free supporting structures in thick film technology: a substrate integrated sensor, in *Proceedings of the 6th European Microelectronics Conference*, 1987, pp. 421-427.

[18]. C. B. Sippola and C. H. Ahn, A ceramic capacitive pressure microsensor with screen-printed diaphragm, in *Proceedings of the 4th IEEE Conference on Sensors*, *2005*, pp. 1271-1274.

[19]. S. Pranonsatit and S. Lucyszyn, Self assembled screen-printed microwave inductors, *Electronics Letters*, Vol. 41, Issue 23, 2005, pp. 1287-1288.

[20]. P. Ginet, C. Lucat, M. Budinger and F. Ménil, New screen-printed thermal microactuator, *IEEE Review on Advances in Micro, Nano, and Molecular Systems,* Vol. 1-3, 2007, pp. 851-855.

[21]. R. Lakhmi, H. Debéda, I. Dufour and C. Lucat, Force sensors based on screen-printed microcantilevers, *IEEE Sensors Journal*, Vol. 10, Issue 6, 2010, pp. 1133-1137.

[22]. C. Castille, C. Lucat, P. Ginet P., F. Ménil, M. Maglione, Free-standing piezoelectric thick-films for MEMS applications, in *Proceedings of the IMAPS/ACerS 4th International Conference on Ceramic Interconnect and Ceramic Microsystems Technologies (IMAPS-CICMT'08)*, Munich, 2008.

[23]. R. Lakhmi, H. Debéda, M. Maglione, I. Dufour and C. Lucat, Study of screen-printed PZT cantilevers both self-actuated and self-read-out, *International Journal of Applied Ceramic Technology*, Vol. 11, Issue 2, 2014, pp. 311-320.

[24]. S. Tétin, B. Caillard, F. Ménil, H. Debéda, C. Lucat, C. Pellet and I. Dufour, Modeling and performance of uncoated microcantilever-based chemical sensors, *Sensors and Actuators B*, Vol. 143, 2010, pp. 555-560.

[25]. R. Lakhmi, H. Debéda, C. Lucat, Uncoated PZT thick film cantilever for chemical species detection in gaseous phase, in *Proceeding of the International Meeting of Chemical Sensors (IMCS'12),* Nuremberg, Germany, 20-23 May 2012.

[26]. M. A. Urbitzondo, A. Peralta, I. Pellejero, J. Sese, M. P. Pina, I. Dufour and J. Santamaria, Detection of organic vapours with Si cantilevers coated with inorganic (zeolites) or organic (polymer) layers, *Sensors and Actuators B*, Vol. 171-172, 2012, pp. 822-831.

[27]. F. J. Arregui, Z. Ciaurriz, M. Oneca and I. R. Matias, An experimental study about hydrogels for the fabrication of optical fiber humidity sensors, *Sensors and Actuators B*, Vol. 96, 2003, pp. 165–172.

[28]. I. Dufour, F. Josse, S. Heinrich, C. Lucat, C. Ayela, F. Ménil, and O. Brand, Unconventional uses of microcantilevers as chemical sensors in gas and liquid media, *Sensors and Actuators B*, 170, 2012, pp. 115-121.